

NASA Technical Memorandum 106839

Finite Difference Time Marching in the Frequency Domain: A Parabolic Formulation for Aircraft Acoustic Nacelle Design

Kenneth J. Baumeister
*Lewis Research Center
Cleveland, Ohio*

and

Kevin L. Kreider
*University of Akron
Akron, Ohio*

Prepared for the
International Mechanical Engineering Congress
and Exposition: The Winter Annual Meeting
sponsored by the American Society of Mechanical Engineers
San Francisco, California, November 12–17, 1995



National Aeronautics and
Space Administration

FINITE DIFFERENCE TIME MARCHING IN THE FREQUENCY DOMAIN: A PARABOLIC FORMULATION FOR AIRCRAFT ACOUSTIC NACELLE DESIGN

Kenneth J. Baumeister
National Aeronautics and Space Administration
Lewis Research Center
Cleveland, Ohio 44135

and

Kevin L. Kreider
The University of Akron
Department of Mathematical Sciences
Akron, Ohio 44325-4002

ABSTRACT

An explicit finite difference iteration scheme is developed to study harmonic sound propagation in aircraft engine nacelles. To reduce storage requirements for large 3D problems, the time dependent potential form of the acoustic wave equation is used. To insure that the finite difference scheme is both explicit and stable, time is introduced into the Fourier transformed (steady-state) acoustic potential field as a parameter. Under a suitable transformation, the time dependent governing equation in frequency space is simplified to yield a parabolic partial differential equation, which is then marched through time to attain the steady-state solution. The input to the system is the amplitude of an incident harmonic sound source entering a quiescent duct at the input boundary, with standard impedance boundary conditions on the duct walls and duct exit. The introduction of the time parameter eliminates the large matrix storage requirements normally associated with frequency domain solutions, and time marching attains the steady-state quickly enough to make the method favorable when compared to frequency domain methods. For validation, this transient-frequency domain method is applied to sound propagation in a 2D hard wall duct with plug flow.

INTRODUCTION

Both steady-state (frequency domain) and transient (time domain) finite difference and finite element techniques have been developed to study sound propagation in aircraft nacelles (Baumeister, 1980a and b and Baumeister and Horowitz 1984). Sound propagation with axial variations in duct geometry, mean flow Mach number and wall sound absorbers have been considered (Astley and Eversman, 1981). To date, the numerical solutions have generally been limited to moderate frequency sound and mean flow Mach numbers in two dimensional axisymmetric nacelles. Wavelength resolution problems have prevented a broader range of applications of the numerical methods. A fine grid is required to resolve the short wavelengths associated with high frequency sound propagation with high inlet

Mach numbers. Thus, application of numerical techniques to high frequency sound propagation in 3-D engine nacelles has yet to be attempted.

Generally, the number of grid points along the centerline of an aircraft nacelle is directly proportional to the sound frequency and the nacelle length and inversely proportional to one minus the mean flow Mach number. In addition, the number of grid points in the transverse direction depends on the radial and spinning mode content of the sound source. These dependencies severely limit the application of numerical techniques.

The present paper is the first step in a larger research effort to develop efficient numerical techniques to predict high frequency sound propagation around 3D aircraft inlet nacelles with large subsonic inlet Mach numbers. The paper begins with a description of the problem, an explanation of why the transient approach is employed, and a description of the grid system and governing equations. The bulk of the paper describes the development of a stable, explicit finite difference scheme by a transformation of the governing hyperbolic wave equation. The scheme is iterated in time to converge to the steady-state solution associated with a Fourier transform solution.

NOMENCLATURE

C dimensionless speed of sound, $C^\# / C_o^\#$, eq. (2)

\bar{c} steady speed of sound, eq. (11)

c' fluctuating speed of sound, eq. (12)

$D^\#$ dimensional duct height or diameter

D duct height, $D = 1$

d parameter, eq. (58)

F source amplitude at duct entrance, eq. (40)
f[#] dimensional frequency
f dimensionless frequency, $f^{\#}D^{\#}/C_0^{\#}$
g parameter, eq. (58)
h parameter, eq. (58)
i $\sqrt{-1}$
L length of duct, $L^{\#}/D^{\#}$, Figure 2
M_f Mach number at duct entrance
n unit outward normal
P[#] dimensional pressure
P dimensionless fluid pressure, $P^{\#}/\rho_0^{\#}C_0^{\#2}$
 \bar{p} steady fluid pressure
P' acoustic pressure fluctuation, eq. (19)
t dimensionless time, $t^{\#}t^{\#}$
t_T total dimensionless calculation time
 Δt time step
u_n[#] normal acoustic velocity, eq. (43)
x dimensionless axial coordinate, $x^{\#}/D^{\#}$
 Δx axial grid spacing
y dimensionless transverse coordinate, $y^{\#}/D^{\#}$
 Δy transverse grid spacing
Z[#] impedance
 γ ratio of specific heats
 ζ dimensionless impedance, $Z^{\#}/\rho_0^{\#}C_0^{\#}$
 ρ dimensionless fluid density, $\rho^{\#}/\rho_0^{\#}$
 $\bar{\rho}$ steady fluid density, eq. (21)
 ρ' fluctuating acoustic density
 Φ dimensionless time dependent flow potential, $\Phi^{\#}/C_0^{\#}D^{\#}$

$\bar{\Phi}$ steady mean flow potential, eq. (5)
 ϕ' transient acoustic potential, eq. (5)
 ϕ transient acoustic potential in frequency space, eq. (30)
 Ψ spatial potential, eq. (28)
 ω dimensionless frequency, $2\pi f$
 ∇ $D^{\#} \nabla^{\#}$

Subscripts

i axial index, see Figure 2
j transverse index, see Figure 2
o ambient or reference condition

Superscript

[#] dimensional quantity
k time step

PROBLEM STATEMENT

The problem under consideration here is the steady-state propagation of sound, represented by the perturbation acoustic potential, through a 2D rectangular duct. The source, noise emanating from fan blades in a jet engine inlet nozzle, is represented by specifying the pressure distribution at the fan face. The goal of the paper is to develop a stable, explicit finite difference scheme that incorporates the far field impedance condition applied at the duct exit and rigid body boundary conditions on the duct walls. The method is designed with the intention of extending the current 2D duct formulation to general 3D nacelle design problems with a variety of possible boundary conditions in the near and far fields.

TRANSIENT APPROACH

In frequency domain approaches, pressure and acoustic velocity are assumed to be harmonic functions of time. The matrices associated with numerical solutions of the governing equations in the frequency domain have extremely large storage requirements. In similar 3D electromagnetic applications, Taflov (1991) reports that frequency domain approaches are limited to several hundred thousand unknowns (still a small problem in 3D). Larger problems encounter roundoff errors and conditioning problems that prevent a reliable solution.

On the other hand, an explicit transient method generates no matrices, and is generally faster than a frequency domain approach (Baumeister, 1980a). Miller has developed explicit relationships showing the time advantage of transient over steady state techniques (Miller, 1988, section V. Some Practical Considerations, C. Discussion). Consequently, the method of choice in the present paper is a time dependent method.

GRID SYSTEM

Three possible mesh systems could be employed to model the time dependent acoustic field in an aircraft nacelle; (1) CFD body fitted grids, (2) unstructured finite element grids and (3) almost highly structured grids. Both the body fitted and finite element grids require extensive storage of information about the grid structure. For 3D problems, this storage requirement places a large burden on available storage and speed of operations. Therefore, the almost highly structure grid is preferred here.

The almost highly structured grid is rectangular away from the geometry of interest, with nonstandard split or stretched finite-volume cells only at the curved surface. Taflove (1991) reports that the processing speed is up to 18 times faster than codes using CFD body-fitted meshes. Furthermore, artifacts due to refraction and reflection of numerical waves propagating across global mesh distortions are reduced.

Figure 1 illustrates an almost structured grid model of an aircraft engine nacelle. Only in the vicinity of the center body or the curved nacelle tip is the grid nonuniform. For the rectangular duct examples considered here, the highly structured grid system shown in Figure 2 is employed.

GOVERNING EQUATIONS

The governing differential equations for studying acoustic propagation in inlet nacelles can be formulated in terms of the constitutive continuity and momentum equations (Baumeister, 1979) or in terms of potential flow (Sigman et. al., 1978). The constitutive equation approach can handle a general 3D sheared flow while the potential approach is limited to 3D inviscid flow. The major advantage of the potential flow approach over the constitutive equation approach comes in decreased storage requirements associated with only one dependent variable.

Fortunately, acoustic propagation in inlet nacelles can be reasonably modeled by an inviscid approximation. For single mode JT15D engine data, a previous finite element study (Baumeister and Horowitz, 1984) employing the potential formulation in the frequency domain showed good agreement with experimental data - in the far field radiation pattern as well as suppressor attenuation. Due to this success, the problem under consideration here is formulated in terms of an acoustic potential.

For inviscid, non heat conducting and irrotational flow, the non-linear partial differential equation for the flow potential can be written in dimensionless form as (Thompson, 1972, pg. 257, eq. 5.24)

$$f^2 \Phi_{tt} + f(\nabla \Phi \cdot \nabla \Phi)_t + \frac{1}{2} \nabla \Phi \cdot \nabla (\nabla \Phi \cdot \nabla \Phi) = C^2 \nabla^2 \Phi \quad (1)$$

where

$$C^2 = 1 - (\gamma - 1) \left(f \Phi_t + \frac{1}{2} \nabla \Phi \cdot \nabla \Phi \right) \quad (2)$$

The symbol Φ represents the time dependent potential of the total flow field. The speed of propagation of a disturbance is represented by C and the frequency of an acoustic source by f . Subscripts indicate partial differentiation with respect to subscripted variables.

The conventional normalization factors used to develop these

nondimensional equations are given in the NOMENCLATURE. However, the normalization of time deserves some special comment. A common choice for normalizing time is $t = C_0 \# t^{\#} / D^{\#}$. The superscript # designates a dimensional quantity while the subscript o indicates an arbitrary reference value. With this choice, the dimensionless frequency f would not appear in eqs. (1) or (2). However, in this paper, the dimensional frequency $f^{\#}$ of the forcing acoustic signal was chosen to normalize time, so that $t = f^{\#} t^{\#}$. As a result, the time t indicates the number of complete acoustic cycles that have occurred since the start of the solution process. This is advantageous because the total time of the numerical calculation can generally be set independently of the frequency of the acoustic signal.

Rewriting eqs. (1) and (2) in two dimensional rectangular coordinates yields:

$$f^2 \Phi_{tt} + f(2\Phi_x \Phi_{xt} + 2\Phi_y \Phi_{yt}) + \Phi_x^2 \Phi_{xx} + 2\Phi_x \Phi_y \Phi_{xy} + \Phi_y^2 \Phi_{yy} = C^2 (\Phi_{xx} + \Phi_{yy}) \quad (3)$$

$$C^2 = 1 - (\gamma - 1) \left(f \Phi_t + \frac{1}{2} \Phi_x^2 + \frac{1}{2} \Phi_y^2 \right) \quad (4)$$

To obtain the acoustic solution, the flow potential is rewritten as the sum of a steady mean flow potential $\bar{\Phi}(x,y)$ and an acoustic potential $\phi'(x,y,t)$; that is

$$\Phi(x,y,t) = \bar{\Phi}(x,y) + \phi'(x,y,t) \quad (5)$$

To simplify the algebra in the linearization of eq. (3), first eq. (4) is linearized and the steady mean flow equation is developed. Substituting eq. (5) into eq.(4) and neglecting second order terms, the speed of the disturbance can be expressed in terms of the steady and fluctuating potentials as

$$C^2 = 1 - (\gamma - 1) \left(f \Phi'_t + \frac{1}{2} \bar{\Phi}_x^2 + \bar{\Phi}_x \phi'_x + \frac{1}{2} \bar{\Phi}_y^2 + \bar{\Phi}_y \phi'_y \right) \quad (6)$$

which can be written in compact form as

$$C^2 = B^2 + B'^2 \quad (7)$$

where

$$B^2 = 1 - \frac{1}{2} (\gamma - 1) (\bar{\Phi}_x^2 + \bar{\Phi}_y^2) \quad (8)$$

$$B'^2 = -(\gamma - 1) (f \phi'_t + \bar{\Phi}_x \phi'_x + \bar{\Phi}_y \phi'_y) \quad (9)$$

To linearize the speed of sound, define

$$C = \bar{c} + c' = \sqrt{B^2 + B'^2} = B \sqrt{1 + \frac{B'^2}{B^2}} \cong B + \frac{1}{2} \frac{B'^2}{B} \quad (10)$$

Therefore, the mean speed of sound depends on the velocity field and can be expressed as

$$\bar{c} = B = \left\{ 1 - \frac{1}{2}(\gamma - 1) \left(\bar{\Phi}_x^2 + \bar{\Phi}_y^2 \right) \right\}^{1/2} \quad (11)$$

while the perturbation of the sonic velocity depends both on the mean flow field and the acoustic field as

$$c' = - \left(\frac{\gamma - 1}{2\bar{c}} \right) \left(f\Phi_t' + \bar{\Phi}_x\phi_x' + \bar{\Phi}_y\phi_y' \right) \quad (12)$$

The differential equation describing the mean flow can now be expressed in terms of the mean sonic velocity. Substituting $\bar{\Phi}$ into both eqs. (3) and (4) yields

$$\bar{\Phi}_x^2 \bar{\Phi}_{xx} + 2\bar{\Phi}_x \bar{\Phi}_y \bar{\Phi}_{xy} + \bar{\Phi}_y^2 \bar{\Phi}_{yy} - \bar{c}^2 (\bar{\Phi}_{xx} + \bar{\Phi}_{yy}) = 0 \quad (13)$$

Now, the linearized wave equation can be conveniently established. Substituting eqs. (5) and (7) into eq.(3), factoring out the steady contribution from eq. (13), and neglecting nonlinear products of the acoustic quantities yields

$$\begin{aligned} 0 = & f^2 \phi_{tt}' - \left(\bar{c}^2 - \bar{\Phi}_x^2 \right) \phi_{xx}' - \left(\bar{c}^2 - \bar{\Phi}_y^2 \right) \phi_{yy}' + 2\bar{\Phi}_x \bar{\Phi}_y \phi_{xy}' \\ & + 2f \bar{\Phi}_x \phi_{xt}' + 2f \bar{\Phi}_y \phi_{yt}' + 2 \left(\bar{\Phi}_x \bar{\Phi}_{xx} + \bar{\Phi}_y \bar{\Phi}_{yy} \right) \phi_x' \\ & + 2 \left(\bar{\Phi}_x \bar{\Phi}_{xy} + \bar{\Phi}_y \bar{\Phi}_{yy} \right) \phi_y' - (\gamma - 1) \\ & \times \left(f \phi_t' + \bar{\Phi}_x \phi_x' + \bar{\Phi}_y \phi_y' \right) \left(\bar{\Phi}_{xx} + \bar{\Phi}_{yy} \right) \end{aligned} \quad (14)$$

For the special case of plug flow, the mean flow terms in eq. (14) become

$$\bar{\Phi}_y = \bar{\Phi}_{xy} = \bar{\Phi}_{xx} = 0 \quad \bar{\Phi}_x = M_f \quad (15)$$

Substituting eq. (15) into eq. (14) yields

$$0 = f^2 \phi_{tt}' - \left(\bar{c}^2 - M_f^2 \right) \phi_{xx}' - \bar{c}^2 \phi_{yy}' + 2f M_f \phi_{xt}' \quad (16)$$

and

$$\bar{c}^2 = 1 - \frac{1}{2} (\gamma - 1) M_f^2 \quad (17)$$

Generally, the pressure at the fan face is specified. Therefore, the relationship between pressure and the potential needs to be determined from the conservation of momentum. The dimensionless form of the conservation of momentum equation can be written as

$$\frac{1}{\rho} P_t = -f \Phi_{tt} - \frac{1}{2} (\nabla \Phi \cdot \nabla \Phi)_t \quad (18)$$

Assuming that

$$P(x, y, t) = \bar{P}(x, y) + P'(x, y, t), \quad (19)$$

$$\rho(x, y, t) = \bar{\rho}(x, y) + \rho'(x, y, t), \quad (20)$$

substituting eqs.(5), (19), and (20) into eq. (18) and neglecting higher order fluctuation terms yields for the acoustic pressure P'

$$\frac{1}{\bar{\rho}} P_t' = -f \phi_{tt}' - \left(\bar{\Phi}_x \phi_x' + \bar{\Phi}_y \phi_y' \right)_t \quad (21)$$

Finally, at the fan face ($x = 0$), assume

$$\bar{\Phi}_y = 0 \quad \text{at } x = 0 \quad (22)$$

$$\bar{\Phi}_x = M_f \quad \text{at } x = 0 \quad (23)$$

and integrate with respect to time to obtain

$$\frac{1}{\bar{\rho}} P'(0, y, t) = -f \phi_t' - M_f \phi_x' \quad (24)$$

Eq. (14) and eq. (24) are the basic equations used to establish a finite difference formulation for the rectangular duct shown in Figure 2. However, care must be taken when discretizing derivative terms to insure that the resulting scheme is both stable and explicit. Note that it is easy to develop a stable implicit method, but this would yield a matrix formulation that is no better than a frequency domain approach. It turns out that the proper treatment of the mixed time and space derivative terms (which appear on the second line of eq. (14)) is critical for maintaining stability.

The implicit formulation is obtained by approximating the mixed partials by (Baumeister, 1980b, eq. (16), and Abramowitz and Stegun, 1964, pg 884, eq. 25.3.27)

$$\phi_{xt}' = \frac{\phi_{i,j}^{k+1} + \phi_{i-1,j}^k + \phi_{i+1,j}^k + \phi_{i,j}^{k-1} - 2\phi_{i,j}^k - \phi_{i-1,j}^{k+1} - \phi_{i+1,j}^{k-1}}{2\Delta x \Delta t} \quad (25)$$

$$\phi_{yt}' = \frac{\phi_{i,j}^{k+1} + \phi_{i,j}^{k-1} + \phi_{i,j+1}^k + \phi_{i,j-1}^k - 2\phi_{i,j}^k - \phi_{i,j+1}^{k+1} - \phi_{i,j-1}^{k-1}}{2\Delta t \Delta y} \quad (26)$$

where i and j denote the space indices for the nodal system shown in Figure 2, k is the time index defined by

$$t^{k+1} = t^k + \Delta t \quad (27)$$

and Δx , Δy , and Δt are the space and time mesh spacings respectively.

Baumeister (1980b) showed that eq. (25) can be used in an explicit fashion for 1D plug flow problems in a duct. However, if the flow is not one dimensional or if the region exterior to the duct is included, the scheme must be implicit. This approach is inappropriate for general 3D problems. Fortunately, this problem can be circumvented by transforming the potential and consequently modifying the governing equation. The details follow in the next section.

TRANSFORMATION TO FREQUENCY SPACE

There are several ways to develop a frequency domain formulation for the general 2D acoustic wave eq. (14) or the plug flow simplification eq. (16). The Fourier Transform can be applied if the potential has a multi-frequency content. In the monochromatic case (Temkin, pg 52, eq. 2.5.1), this is equivalent to assuming that

$$\phi'(x, y, t) = \Psi(x, y) e^{-i\omega^* t^*} = \Psi(x, y) e^{-i2\pi t} \quad (28)$$

which, in the case of plug flow (from eq. (16)), yields

$$0 = (\bar{c}^2 - M_f^2) \Psi_{xx} + \bar{c}^2 \Psi_{yy} + \omega^2 \Psi + i2\omega M_f \Psi_x \quad (29)$$

This equation would be solved numerically using a linear system of equations. However, the associated matrix is not positive definite, which can lead to numerical difficulties, and which preclude the use of iterative techniques (see TRANSIENT APPROACH). Therefore, it is desirable to develop an explicit finite difference scheme to avoid the use of matrices. The situation is complicated by the fact that boundary conditions can introduce instabilities (Baumeister, 1982 and Cabelli, 1982) in the solution process. In time-dependent form, eq. (14) or (16) cannot easily be discretized in such a way that the resulting finite difference scheme is both stable and explicit in the presence of flow (it is possible to obtain reasonable results in the no-flow case).

The resolution of these difficulties is achieved by modifying the monochromatic transformation (28) to

$$\phi'(x, y, t) = \phi(x, y, t) e^{-i\omega^* t^*} = \phi(x, y, t) e^{-i2\pi t} \quad (30)$$

This differs from the classical monochromatic transformation in that the amplitude ϕ (no prime) is no longer assumed to be independent of time, as in eq. (28). Employing eq. (30), the time derivatives in eqs. (14) and (16) can be replaced by the following relationships:

$$\phi'_t = [-i2\pi\phi + \phi_t] e^{-i2\pi t} \quad (31)$$

$$\phi'_{xt} = [-i2\pi\phi_x + \phi_{xt}] e^{-i2\pi t} \quad (32)$$

$$\phi''_{tt} = \frac{\partial}{\partial t}(\phi'_t) = (\phi_{tt} - 2i2\pi\phi_t - (2\pi)^2\phi) e^{-i2\pi t} \quad (33)$$

Under this transformation, the general equation (14) and the plug flow equation (16) become, respectively

$$\begin{aligned} f^2 \phi''_{tt} - [i2f\omega + (\gamma - 1)f(\bar{\Phi}_{xx} + \bar{\Phi}_{yy})] \phi'_t + 2f\bar{\Phi}_x \phi_{xt} \\ + 2f\bar{\Phi}_y \phi_{yt} = (\bar{c}^2 - \bar{\Phi}_x^2) \phi_{xx} + (\bar{c}^2 - \bar{\Phi}_y^2) \phi_{yy} \\ - 2\bar{\Phi}_x \bar{\Phi}_y \phi_{xy} + \omega^2 \phi + i2\omega \bar{\Phi}_x \phi_x + i2\omega \bar{\Phi}_y \phi_y \\ - 2(\bar{\Phi}_x \bar{\Phi}_{xx} + \bar{\Phi}_y \bar{\Phi}_{yy}) \phi_x - 2(\bar{\Phi}_x \bar{\Phi}_{xy} + \bar{\Phi}_y \bar{\Phi}_{yx}) \\ \times \phi_y + (\gamma - 1)(-i\omega\phi + \bar{\Phi}_x \phi_x + \bar{\Phi}_y \phi_y)(\bar{\Phi}_{xx} + \bar{\Phi}_{yy}) \end{aligned} \quad (34)$$

$$\begin{aligned} f^2 \phi''_{tt} - 2if\omega\phi_t + 2fM_f \phi_{xt} = (\bar{c}^2 - M_f^2) \phi_{xx} \\ + \bar{c}^2 \phi_{yy} + \omega^2 \phi + i2\omega M_f \phi_x \end{aligned} \quad (35)$$

To see the relationship between the two transforms (eq. (28) and (30)), consider, for simplicity, the case of plug flow. The monochromatic transform yields eq. (29), while the transient transformation yields eq. (35). The only difference is in the presence of the time derivative terms on the left hand side of eq. (35). Physically, the time dependence in $\phi(x, y, t)$ is caused by assuming that the duct is quiescent at time 0, and that the source is turned on at that instant. A series of numerical calculations was performed to investigate the relationship between ψ and ϕ as time progresses. It was verified that ϕ converges to the steady state ψ , so that

$$\lim_{t \rightarrow \infty} \phi(x, y, t) = \Psi(x, y) \quad (36)$$

At present, a formal proof of convergence is not available.

At present, transient solutions in frequency space are of no interest. Therefore, approximations to eqs. (34) or (35) can be made, by modifying the time derivative terms, as long as the following two factors are taken into account: 1) the resulting scheme must be both stable and explicit, and 2) there must be at least one time derivative term in the equation to ensure that the scheme can be marched through time to obtain the steady state solution. The mixed space-time derivative term in eq. (35) prevents an explicit finite difference representation of the governing equation, and is therefore dropped. Furthermore, the hyperbolic time term in eq. (35) is also dropped to further simplify the governing equation. For plug flow, this produces a parabolic "wave" equation of the form:

$$-2if\omega\phi_t = (\bar{c}^2 - M_f^2) \phi_{xx} + \bar{c}^2 \phi_{yy} + \omega^2 \phi + i2\omega M_f \phi_x \quad (37)$$

This type of differential manipulation is often associated with preconditioning of both time dependent partial differential equations (Turek, Fiterman and Leer, 1994) and time independent partial differential equations (Turek and Arnone, 1993) to accelerate convergence to the steady state solution. Here, though, the goal is obtaining a stable, explicit scheme.

In the absence of mean flow, the parabolic wave equation takes on

the form

$$-2i\omega\phi_t = \phi_{xx} + \phi_{yy} + \omega^2\phi \quad (38)$$

The right hand side of eq. (38) becomes the Helmholtz equation. In the Fourier transform approach, Bayliss, Goldstein, and Turkel (1982) have developed an iterative approach to its associated matrix; however, the Gaussian elimination approach is still the method of choice. In effect, the time iteration procedure presented in this paper offers a very simple iterative solution to this classic equation.

INITIAL AND BOUNDARY CONDITIONS

The duct is assumed to be quiescent at time 0, so that the initial condition is

$$\phi(x, y, 0) = 0 \quad (39)$$

As the equation is iterated in time, the solution builds up to the steady state solution.

At the duct entrance, ($x=0$), the potential is given by

$$\phi'(0, y, t) = F(y)e^{-i2\pi t} \quad (40)$$

and through eq. (30) to

$$\phi(0, y, t) = F(y) \quad (41)$$

If the pressure at $x=0$ is specified as the boundary condition, then the potential is related to the pressure directly through eq. (24).

The wall and exit boundary conditions in hyperbolic space generally require special considerations. Rigorous treatment of time dependent boundary conditions for hyperbolic systems is quite involved (Thompson, 1987). In time dependent duct propagation problems, impedance concepts have generally not proven useful (Banks, Propst and Silcox, 1991). However, in the frequency formulation, Baumeister & Horowitz (1984) found impedance concepts very useful in describing the operation of real jet engine noise suppressors. Thus, a major advantage of the transient-frequency formulation presented here is the capability of using the impedance and gradient conditions as developed for the frequency domain.

The hard wall condition is

$$\nabla\phi \cdot \mathbf{n} = 0 \quad (42)$$

where \mathbf{n} is the unit outward normal.

To simulate a non-reflective boundary at the duct exit, the difference equation is expressed in terms of an exit impedance. For the examples presented in this paper, the duct exit impedance is taken to be that for a plane acoustic wave. The impedance $Z^\#$ is defined as (Skudrzyk, eq. (34) section 15.4, pg. 299)

$$Z^\# = \frac{P'^\#}{u_n'^\#} = \frac{P'^\#}{\nabla\phi'^\# \cdot \mathbf{n}} \quad (43)$$

where $P'^\#$ is the acoustic pressure at the interface and $u_n'^\#$ is the

component of the particle velocity normal to its surface, pointing into the medium characterized by $Z^\#$. The velocity $u_n'^\#$ is positive if its direction points into the second medium, i.e., to the outside of the surface that contains the incident wave.

In dimensionless form, eq. (43) can be written as

$$\zeta = \frac{Z^\#}{\bar{\rho}^\# c_o^\#} = \frac{P'}{\frac{\partial\phi'}{\partial x}} \quad (44)$$

Substituting in the relationship between pressure and potential for plug flow as given in eq. (24) yields

$$\zeta = -\bar{\rho} \frac{[f\phi'_t + M_f\phi'_x]}{\phi'_x} \quad (45)$$

or

$$\phi'_x = \frac{-f\phi'_t}{\zeta + M_f} \quad (46)$$

Since the equations are being developed for harmonic flow, the following relationship can be used to simplify eq. (46):

$$\phi'_t \Big|_{t \rightarrow \infty} = -i2\pi\phi e^{-i2\pi t} \quad (47)$$

Therefore, the relationship between the gradient of ϕ and the impedance in eq. (46) can be written as

$$\phi_x = \frac{i\omega}{\zeta + M_f} \phi \quad (48)$$

For plane wave propagation, the plug flow solution for the acoustic potential is

$$\phi'(x, t) = e^{\frac{i\omega}{\bar{c} + M_f} x} e^{-i2\pi t} \quad (49)$$

Substituting eq. (49) into eq. (45) yields

$$\zeta = \bar{\rho} \bar{c} \quad (50)$$

Substituting eq. (50) into eq. (48) gives the value of the exit gradient at the end of the finite difference domain:

$$\phi_x = \frac{i\omega}{\bar{c} + M_f} \phi \quad (51)$$

This gradient is used to simulate the non-reflective exit condition.

This approach can be used only to simulate plane waves in ducts or at a termination deep in the far field from an engine nacelle. For multimode propagation in ducts or grid termination in the near field, the modal-element method has been found to be very useful. That method can be used within this transient-frequency framework. In

acoustics, Astley and Eversman (1981) and Baumeister and Kreider (1993) applied the modal element method to duct acoustic and scattering problems. In conventional CFD, Baumeister and Baumeister (1994) also applied the method to potential flow over a cylinder within a duct.

FINITE DIFFERENCE EQUATIONS

The finite difference approximations determine the potential at the spatial grid points at discrete time steps $t^k = k\Delta t$. Starting from the known initial conditions at $t = 0$ and the boundary conditions, the algorithm marches the solution out to later times.

Away from the duct boundaries, as shown by the cell in Figure 2, each partial derivative in eq. (37) can be expressed as follows:

$$\phi_t = \frac{\phi_{i,j}^{k+1} - \phi_{i,j}^{k-1}}{2\Delta t} \quad (52)$$

$$\phi_{xx} = \frac{\phi_{i+1,j}^k - 2\phi_{i,j}^k + \phi_{i-1,j}^k}{\Delta x^2} \quad (53)$$

$$\phi_{yy} = \frac{\phi_{i,j+1}^k - 2\phi_{i,j}^k + \phi_{i,j-1}^k}{\Delta y^2} \quad (54)$$

$$\phi_x = \frac{\phi_{i+1,j}^k - \phi_{i-1,j}^k}{2\Delta x} \quad (55)$$

$$\phi = \phi_{i,j}^k \quad (56)$$

Substituting these expressions into eq. (37) yields

$$\begin{aligned} \phi_{i,j}^{k+1} \left(\frac{-h}{\Delta t} \right) &= \phi_{i,j}^k \left(-\frac{2d^2}{\Delta x^2} - \frac{2\bar{c}^2}{\Delta y^2} \right) + \phi_{i+1,j}^k \left(\frac{d^2}{\Delta x^2} + \frac{g}{2\Delta x} \right) \\ &+ \phi_{i-1,j}^k \left(\frac{d^2}{\Delta x^2} - \frac{g}{2\Delta x} \right) + \phi_{i,j+1}^k \left(\frac{\bar{c}^2}{\Delta y^2} \right) \\ &+ \phi_{i,j-1}^k \left(\frac{\bar{c}^2}{\Delta y^2} \right) + \phi_{i,j}^{k-1} \left(\frac{-h}{\Delta t} \right) + \omega^2 \phi_{i,j}^k \end{aligned} \quad (57)$$

where

$$\begin{aligned} d^2 &= \bar{c}^2 - M_f^2 \\ h &= i\omega f \\ g &= 2i\omega M_f \end{aligned} \quad (58)$$

Eq. (57) is an explicit two step scheme. At $t = 0$, field values at t^{k-1} are assumed zero because the initial field is quiescent.

The expressions for the difference equations at the boundaries are complicated somewhat by the impedance conditions. However, a simple integration procedure resolves this problem. Baumeister

(1980a & 1980b) gives precise details for generating the time difference equations at the boundaries.

STABILITY

A von Neumann stability analysis (Lapidus and Pinder, 1982) indicates that the method is conditionally stable, subject to the conservative condition

$$\Delta t < \frac{1}{\omega f \left[\left(\frac{d}{\Delta x} \right)^2 + \left(\frac{\bar{c}}{\Delta y} \right)^2 \right] - \pi + \frac{|M_f|}{f \Delta x}} \quad (59)$$

In a typical application, ω , f , and M_f are set by the engine operating conditions. Next, the grid spacing parameters Δx and Δy are set to accurately resolve the estimated spatial harmonic variation of the acoustic field. Finally, Δt is chosen to satisfy eq. (59).

In the von Neumann analysis, conditional stability means that the amplification factor, which describes how errors propagate from one time step to the next, has magnitude one. Thus, when inequality (59) is satisfied, errors are not magnified or diminished in magnitude. This is a desirable property, since the numerical formulation can not distinguish between an error and a small acoustic mode.

The von Neumann stability analysis does not take into account boundary conditions. For stability, gradient boundary conditions require the use of smaller Δt than predicted by inequality (eq. (59)).

NUMERICAL EXAMPLES

In the three examples that follow, the parabolic transient-frequency domain results are compared to the exact results of the steady Fourier transformed solutions, given by eq. (49).

The following problem is considered: a plane wave propagates from the left into a quiescent duct of length one, and the acoustic potential field is to be computed in the duct. Note that, boundary conditions can introduce instabilities (Baumeister, 1982 and Cabelli, 1982) into otherwise stable finite difference schemes. Therefore, it is important to test the proposed method for convergence in time to the steady state solution in the absence of the exit boundary condition (eq. (51)), and to test independently the effect of the exit boundary condition itself on the solution.

Semi-Infinite Duct

In this example, the computational boundary is set far enough away from the true boundary $x=1$ that any artifacts arising from imperfections in the exit boundary condition do not affect the solution in $[0,1]$. The numerical solution propagates one node per time step, so setting the boundary at $x=50$ with step $\Delta x=0.05$ provides a sufficient number of time steps to gauge the convergence of the method before any artifacts might reflect back from the computational boundary.

The numerical and exact results are compared in Figure 3, for no flow (Fig. 3a) and for Mach number $M_f = -0.5$ (Fig. 3b). The frequency is normalized to $f=1$. Both cases show excellent agreement. The total calculation time was $t_T=5.0$.

Finite Duct $L=1$

In this example, the computational boundary is moved up to the true boundary $x=1$ to examine the effect of the exit boundary condition (eq. (51)). The frequency is normalized to 1. Again, two cases were considered - no flow ($M_f = 0$) and Mach number $M_f=-0.5$. The results are shown in Figure 4a and 4b, respectively. The numerical results again match well with the exact results, but it is clear that the exit boundary condition does have a slight degrading effect on the solution. Notice also that the time step has been decreased here, which tends to increase the execution time; however, the computational domain is smaller, which tends to decrease the execution time. The total calculation time in this example was $t_T = 4.0$.

CONVERGENCE RATE

In this example, the convergence rate is studied for the region $x = 0$ to $x = 1$ using the semi-infinite duct. The results are shown in Figure 5 for the real and imaginary components of the potential and Figure 6 for the magnitude of the potential. As seen in these figures, the numerical solution quickly and accurately converges to the exact steady state solution.

For this plane wave propagation, the exact solution to the hyperbolic governing equations predicts the arrival of the "steady state" solution when $t=1$ (Baumeister, 1983, eq. (28) renormalized). As seen in Figures 5 and 6, the parabolic solutions converges to the Fourier transformed results after a time of $t=2$ has elapsed. Thus, the parabolic marching scheme requires more time steps to converge than a hyperbolic method.

For parabolic partial differential equations with real coefficients, disturbances propagate with infinite speed (Morse and Feshbach, 1953, pg. 865). In the present calculations, numerical solutions to the parabolic eq. (37) have this trait. The finite difference values of the potential propagate throughout the domain at the numerical velocity $\Delta x/\Delta t$ rather than the speed of sound. This characteristic may account for the slower convergence time for the parabolic formulation as compared to the hyperbolic formulation of the appropriate governing equations. In the parabolic scheme, acoustic energy is numerically transferred ahead of the true wave front. Nevertheless, the parabolic scheme provides the correct steady state solution using minimal computer storage with run times comparable to other methods.

HISTORICAL PERSPECTIVE

With the transient-frequency approach developed in this paper, three different finite difference/element solution techniques are now available to solve the hyperbolic wave equation that describes acoustic propagation in jet engine nacelles. This is outlined in Figure 7 for the zero mean flow case.

The Fourier transform of the wave equation was the first numerical approach used to study sound propagation in jet engine ducts (Baumeister and Bitner, 1973 and Baumeister and Rice, 1973). This steady state approach is outlined on the right side of Figure 7. The governing hyperbolic wave equation is transformed to the elliptic Helmholtz equation. Finite difference (FD) and finite element (FE) numerical formulations have been employed to solve this equation. After applications of the boundary conditions (Fig. 7; [BC]), the associated finite difference or finite element global matrix is solved

for the velocity potential (or pressure). Because the matrix form of the Helmholtz equation is not positive definite, matrix elimination solutions are generally employed. This requires extensive storage, as discussed in TRANSIENT APPROACH. Conveniently, the steady state approach allows the direct calculation of the potential (or pressure) fields.

In the inlet to a turbojet engine, the dimensionless frequencies f can be on the order of 30 to 50 for the higher harmonics of the blade passing frequency. The storage requirements and associated computer run times for these high frequencies make computations expensive or even impossible. To make the numerical solutions more cost effective, grid saving approximations to the governing Helmholtz equation have been used (Fig. 7; [Approximate]). Baumeister (1974) employed the wave envelope theory while Hardin and Tappert (1973) developed a similar approach for underwater sound propagation with the addition of a parabolic (space) approximation. Candel (1986) presents an extensive discussion of the contemporary research in this area and a detailed development of the parabolic equation method (PEM).

The transient solution to the wave equation was the second numerical approach used to study propagation in jet engine ducts, which is shown in the left-hand column of Figure 7. To eliminate the matrix storage requirements, Baumeister developed time dependent finite difference numerical solutions for noise propagation in a two-dimensional duct without flow (1980a), with parallel shear flow (1979) and with axisymmetric flow (1980b).

Sound is introduced as a boundary condition at the duct entrance. The initial conditions generally assume a quiescent duct. Finite difference (FD) approximations to the hyperbolic wave equation are then solved by an iteration process. The calculations are run until the initial transience dies out and steady harmonic oscillations are established. Finally, the transient variable ϕ' is transformed into the steady state variable ψ associated with the solution of the Helmholtz equation. As with the steady state approach, simplification to the governing equations (Fig. 7; [Approximations]) can reduce computer storage and run times (Baumeister, 1986).

The third option, the transient-frequency technique, is illustrated in the central column of Figure 7. This fully explicit iteration method eliminates the large matrix storage requirements of steady state techniques and allows the use of conventional impedance conditions. As time increases, the iteration process directly computes the steady state variable ψ .

CONCLUDING REMARKS

A transient-frequency domain numerical solution of the potential acoustic equation has been developed. The potential form of the governing equations has been employed to reduce the number of dependent variables and their associated storage requirements. This fully explicit iteration method represents a significant advance over previous steady state and transient techniques. Time is introduced into the steady state formulation to form a hyperbolic equation. A parabolic approximation (in time) to this hyperbolic equation is employed. The field is iterated in time from an initial value of 0 to attain the steady state solution.

The method eliminates the large matrix storage requirements of steady state techniques in the frequency domain but still allows the use of conventional impedance conditions. Most importantly, the formulation is fully explicit under flow conditions. In each example

provided, the numerical solution quickly and accurately converges to the exact steady state solution.

REFERENCES

- Abramowitz, M. and Stegun, I. A., 1964, Handbook of Mathematical Functions With Formulas, Graphs, and Mathematical Tables, National Bureau of Standards Applied Mathematics.
- Astley, R. J. and Eversman, W., 1981, "Acoustic Transmission in Non-Uniform Ducts with Mean Flow, Part II: The Finite Element Method," *Journal of Sound and Vibration*, Vol. 74, pp. 103-121.
- Banks, H. T., Propst, G. and Silcox, R. J., 1991, "A Comparison of the Time Domain Boundary Conditions For Acoustic Waves in Waves Guides," ICASE Report No. 91-27, NASA Langley, Hampton, Virginia.
- Baumeister, K. J. and Bittner, E. C., 1973, "Numerical Simulation of Noise Propagation in Jet Engine Ducts", NASA TN-7339.
- Baumeister, K. J., 1974, "Analysis of Sound Propagation in Ducts Using the Wave Envelope Concept," NASA TN D-7719, 1974
- Baumeister, K. J. and Rice, E. J., 1975, "A Difference Theory for Noise Propagation in an Acoustically Lined Duct with Mean Flow," *Aeroacoustics: Jet and Combustion Noise; Duct Acoustic*, H. T. Nagamatsu, J. V. O'Keefe, and I. R. Schwartz, eds., *Progress in Astronautics and Aeronautics Series*, Vol. 37, American Institute of Aeronautics and Astronautics, New York, 1975, pp. 435-453.
- Baumeister, K. J., 1979, "A Time Dependent Difference Theory For Sound Propagation in Ducts with Flow," paper presented at 98th meeting of the Acoustical Society of America, Salt Lake City, Utah (also NASA TM 79302).
- Baumeister, K. J., 1980a, "Time-Dependent Difference Theory for Noise Propagation in a Two-Dimensional Duct," *AIAA Journal* Vol. 18, No. 12, pp. 1470.
- Baumeister, K. J., 1980b, "Time-Dependent Difference Theory for Sound Propagation in Axisymmetric Ducts with Plug Flow, paper AIAA-80-1017, Hartford, Connecticut.
- Baumeister, K. J., 1982, "Influence of exit impedance on finite-difference solutions of transient acoustic mode propagation in ducts," *ASME Jour. of Engineering for Industry* 104, 113-120.
- Baumeister, K. J. and Horowitz, S. J., 1984, "Finite Element-Integral Acoustic Simulation of JT15D Turbofan Engine, *J. of Vibration, Acoustics, Stress and Reliability in Design*, Vol. 106, pg. 405.
- Baumeister, K. J., 1986, "Time Dependent Wave Envelope Finite Difference Analysis of Sound Propagation," *AIAA Journal* Vol. 24 No 1, pp. 32-38.
- Baumeister, K. J. and Baumeister, J. F., 1994, "Modal Element Method for Potential Flow in Non-Uniform Ducts: Combining Closed Form Analysis With CFD," AIAA paper 94-0813.
- Baumeister, K. J. and Kreider, K. L., 1993, "Modal Element Method for Scattering of Sound by Absorbing Bodies," *Transactions of the ASME, Jour. Vibrations and Acoustics*, Vol. 115, p 314-323.
- Bayliss, A., Goldstein, C. I. and Turkel, E., "An Iterative Method for the Helmholtz Equation," *Journal of Computational Physics*, 49: 443-457, 1983.
- Cabelli, A., 1982, "Duct acoustics - A time dependent difference approach for steady state solutions," *J. Sound & Vibrations* 85, 423-434.
- Candel, S. M., 1986, "A Review of Numerical Methods in Acoustic Wave Propagation," *Recent Advances in Aeroacoustics*, Edited by Krothapalli, A. and Smith C. A., Springer-Verlag, New York.
- Lapidus, L. and Pinder, G. F., 1982, "Numerical Solution of Partial of Partial Differential Equations in Science and Engineering," Wiley-Interscience, New York.
- Miller, E. K., 1988, "A Selective Survey of Computational Electromagnetics", *IEEE Trans. on Antennas and Propagation*, Vol. 36, No. 9, pg. 1281.
- Morse, P. M. and Feshbach, H., "Method of Theoretical Physics," McGraw-Hill, New York, 1953.
- Sigman, R. K., Majjigi, R. K., and Zinn, B. T., 1978, "Determination of Turbofan Inlet Acoustics Using Finite Elements," *AIAA Journal*, Vol. 16, No. 11, Nov., pp. 1113-1145.
- Skudrzyk, E., 1971, "The Foundations of Acoustics," Springer-Verlag, New York.
- Taflove, A., 1991, "Finite-Difference Time-Domain Modeling of Electrically Large Ducts", High Frequency Electromagnetic Jet Engine Cavity Modeling Workshop, WL/AARA & AFIT/ENG Wright-Patterson AFB Ohio.
- Temkin, S., 1981, "Elements of Acoustics," John Wiley & Sons, New York.
- Thompson, K. W., 1987, "Time Dependent Boundary Conditions for Hyperbolic Systems," *Journal of Computational Physics* 68, 1-24 (1987).
- Thompson, P. A., 1972, "Compressible-Fluid Dynamics", McGraw-Hill.
- Turkel, E. and Arnone, A., "Pseudo-Compressibility Methods for the Incompressible Flow Equations," *Proceedings 11th AIAA Computational Fluid Dynamics Conference*, 349-357, AIAA paper 93-3329, 1993.
- Turkel, E., Fiterman, A. and van Leer, B., "Preconditioning and the Limit of the Compressible to the Incompressible Flow Equations for Finite Difference Schemes," *Computing the Future: Advances and Prospects for Computational Aerodynamics* ed. M. Hafez and D.A. Caughey, John Wiley and Sons, 1994.

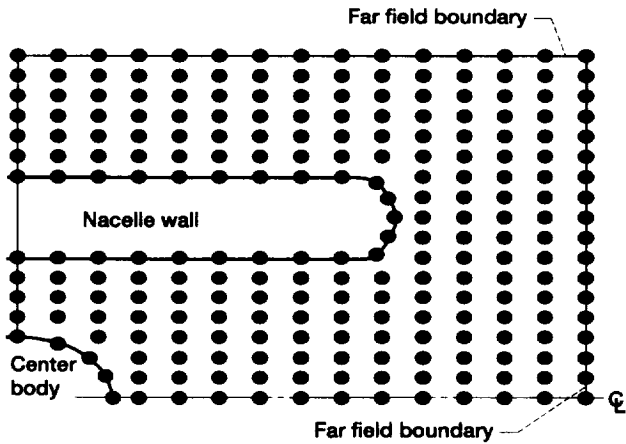


Figure 1.—Almost-completely structured FD-TD mesh for aircraft inlet acoustic nacelle model.

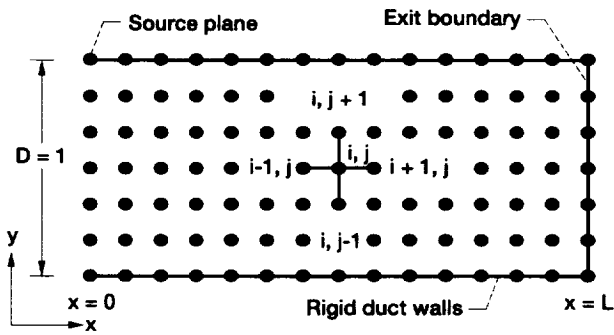


Figure 2.—Structured FD-TD mesh for rectangular duct.

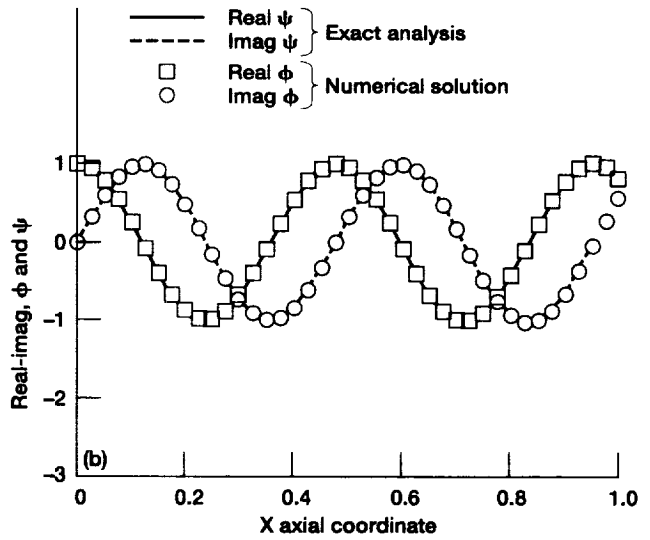
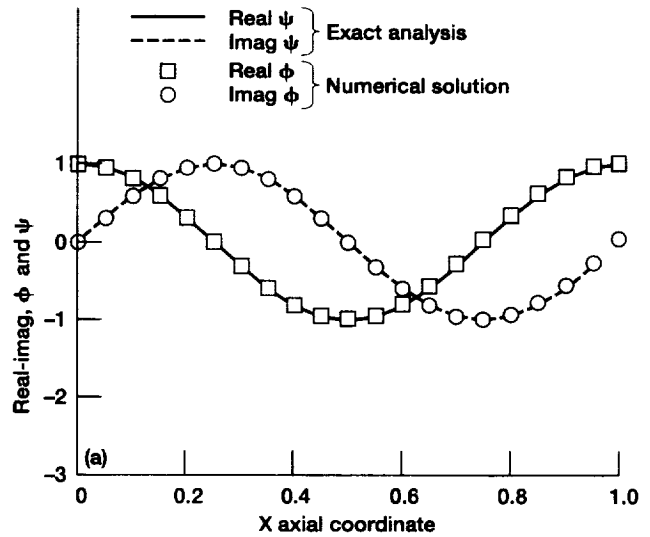


Figure 3.—Analytical and numerical potential profiles along wall for plane wave propagating in a semi-infinite hard wall duct ($f = 1$). (a) $M_f = 0$ ($\Delta x = 0.05$, $\Delta t = 0.003$, $t_T = 5.0$). (b) $M_f = -0.5$ ($\Delta x = 0.025$, $\Delta t = 0.001$, $t_T = 5.0$).

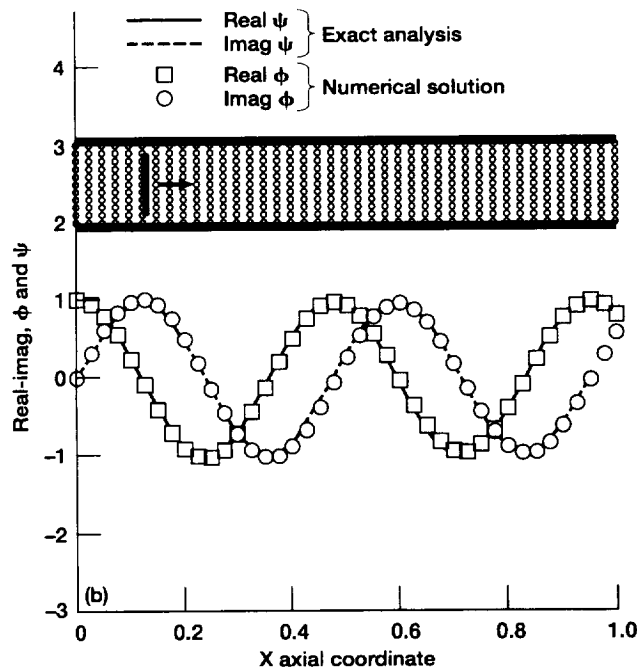
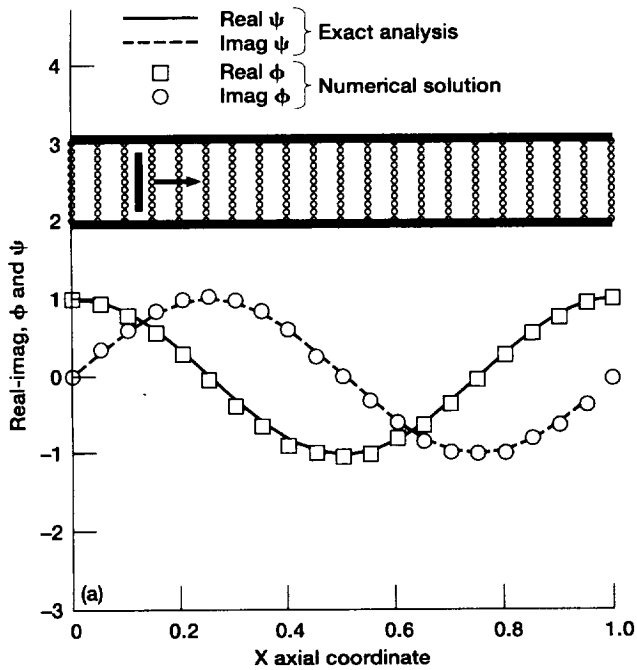


Figure 4.—Analytical and numerical potential profiles along wall for plane wave propagating in a hard wall duct of unit length and a non-reflecting exit condition ($f = 1$). (a) $M_f = 0$ ($\Delta x = 0.05$, $\Delta t = 0.0001$, $\tau_T = 4.0$). (b) $M_f = -0.5$ ($\Delta x = 0.025$, $\Delta t = 0.00001$, $\tau_T = 4.0$).

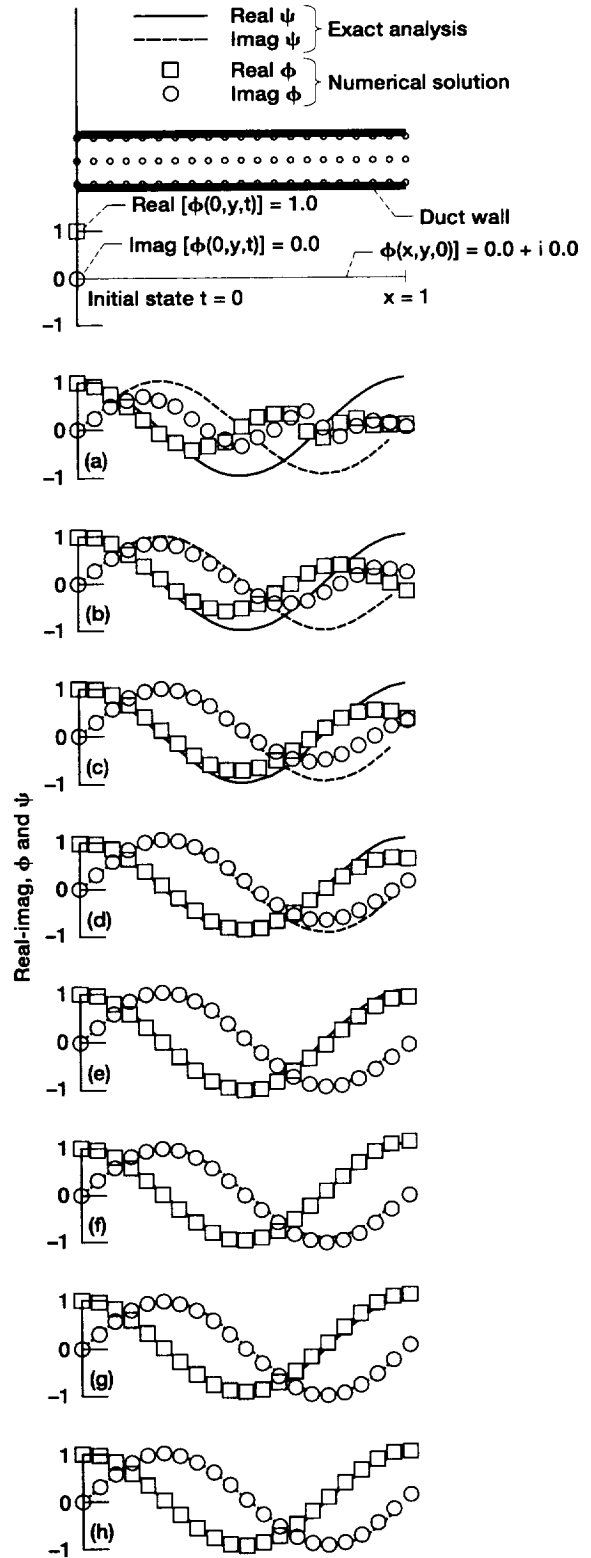


Figure 5.—Developing history of disturbance propagation in Fourier transformed domain as a function of time. ($M_f = 0$, $\Delta x = 0.05$, $\Delta t = 0.0003$). (a) $t = 0.25$. (b) $t = 0.5$. (c) $t = 0.75$. (d) $t = 1.00$. (e) $t = 1.5$. (f) $t = 2.0$. (g) $t = 2.5$. (h) $t = 3.0$.

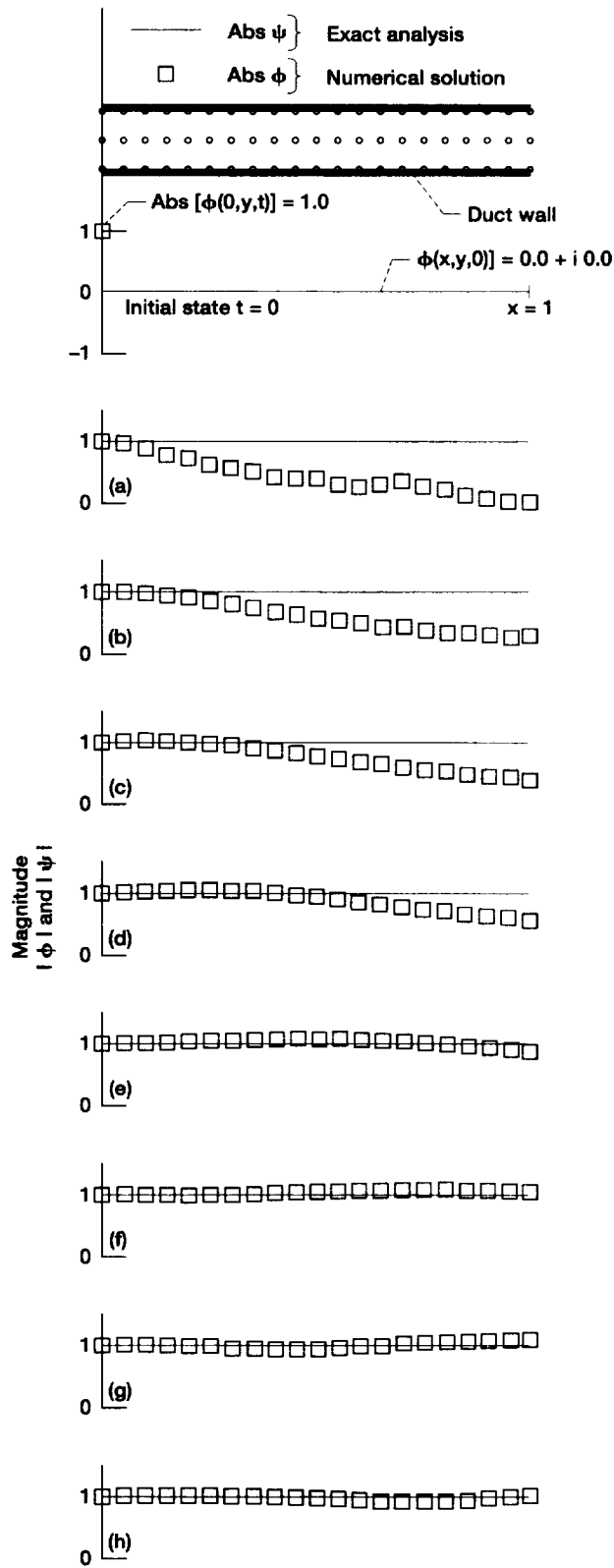


Figure 6.—Developing history of magnitude of disturbance propagation in Fourier transformed domain as a function of time. ($M_f = 0$, $\Delta x = 0.05$, $\Delta t = 0.003$). (a) $t = 0.25$. (b) $t = 0.5$. (c) $t = 0.75$. (d) $t = 1.00$. (e) $t = 1.5$. (f) $t = 2.0$. (g) $t = 2.5$. (h) $t = 3.0$.

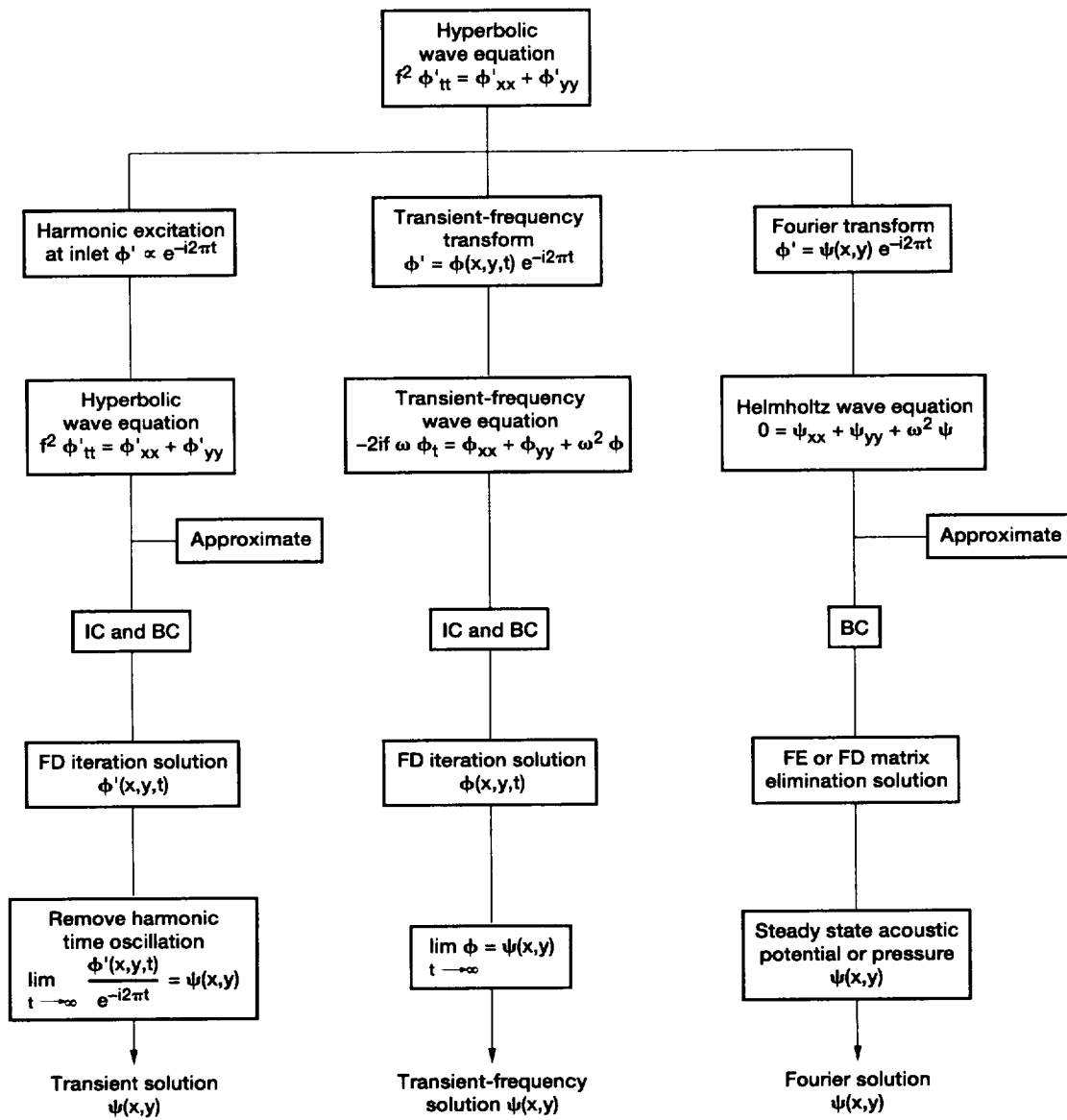


Figure 7.—Alternate finite difference/element methods in solving wave equations.

REPORT DOCUMENTATION PAGE

Form Approved
OMB No. 0704-0188

Public reporting burden for this collection of information is estimated to average 1 hour per response, including the time for reviewing instructions, searching existing data sources, gathering and maintaining the data needed, and completing and reviewing the collection of information. Send comments regarding this burden estimate or any other aspect of this collection of information, including suggestions for reducing this burden, to Washington Headquarters Services, Directorate for Information Operations and Reports, 1215 Jefferson Davis Highway, Suite 1204, Arlington, VA 22202-4302, and to the Office of Management and Budget, Paperwork Reduction Project (0704-0188), Washington, DC 20503.

1. AGENCY USE ONLY (Leave blank)		2. REPORT DATE September 1996	3. REPORT TYPE AND DATES COVERED Technical Memorandum	
4. TITLE AND SUBTITLE Finite Difference Time Marching in the Frequency Domain: A Parabolic Formulation for Aircraft Acoustic Nacelle Design			5. FUNDING NUMBERS WU-505-62-52	
6. AUTHOR(S) Kenneth J. Baumeister and Kevin L. Kreider				
7. PERFORMING ORGANIZATION NAME(S) AND ADDRESS(ES) National Aeronautics and Space Administration Lewis Research Center Cleveland, Ohio 44135-3191			8. PERFORMING ORGANIZATION REPORT NUMBER E-9403	
9. SPONSORING/MONITORING AGENCY NAME(S) AND ADDRESS(ES) National Aeronautics and Space Administration Washington, D.C. 20546-0001			10. SPONSORING/MONITORING AGENCY REPORT NUMBER NASA TM-106839	
11. SUPPLEMENTARY NOTES Prepared for the International Mechanical Engineering Congress and Exposition: The Winter Annual Meeting sponsored by the American Society of Mechanical Engineers, San Francisco, California, November 12-17, 1995. Kenneth J. Baumeister, NASA Lewis Research Center; Kevin L. Kreider, University of Akron, Department of Mathematical Sciences, Akron, Ohio 44325-4002. Responsible person, Kenneth J. Baumeister, organization code 2660, (216) 433-5886.				
12a. DISTRIBUTION/AVAILABILITY STATEMENT Unclassified - Unlimited Subject Category 71 This publication is available from the NASA Center for Aerospace Information, (301) 621-0390.			12b. DISTRIBUTION CODE	
13. ABSTRACT (Maximum 200 words) An explicit finite difference iteration scheme is developed to study harmonic sound propagation in aircraft engine nacelles. To reduce storage requirements for large 3D problems, the time dependent potential form of the acoustic wave equation is used. To insure that the finite difference scheme is both explicit and stable, time is introduced into the Fourier transformed (steady-state) acoustic potential field as a parameter. Under a suitable transformation, the time dependent governing equation in frequency space is simplified to yield a parabolic partial differential equation, which is then marched through time to attain the steady-state solution. The input to the system is the amplitude of an incident harmonic sound source entering a quiescent duct at the input boundary, with standard impedance boundary conditions on the duct walls and duct exit. The introduction of the time parameter eliminates the large matrix storage requirements normally associated with frequency domain solutions, and time marching attains the steady-state quickly enough to make the method favorable when compared to frequency domain methods. For validation, this transient-frequency domain method is applied to sound propagation in a 2D hard wall duct with plug flow.				
14. SUBJECT TERMS Finite difference; Wave equation; Potential transient			15. NUMBER OF PAGES 15	
			16. PRICE CODE A03	
17. SECURITY CLASSIFICATION OF REPORT Unclassified	18. SECURITY CLASSIFICATION OF THIS PAGE Unclassified	19. SECURITY CLASSIFICATION OF ABSTRACT Unclassified	20. LIMITATION OF ABSTRACT	